Numerical investigation of turbulent double-diffusive mixed convection in a slot ventilated enclosure with supply air flow ports

L. KOUFI [a, b, c], Z. YOUNSI [b, c], H. NAJI [a, c]

[a] Univ. Artois, Laboratoire de Génie Civil et géo-Environnement (LGCgE - EA 4515), F-62400 Béthune, France, hassane.naji@univ-artois.fr

[b] FUPL, Hautes Études d'Ingénieur, LGCgE - EA 4515, 13 Rue de Toul, F-59000 Lille, France, zohir.younsi@yncrea.fr & lounes.koufi@yncrea.fr

[c] Univ. Lille Nord de France, LGCgE - EA 4515, F-59000 Lille, France

Abstract:

A numerical study has been achieved for turbulent double-diffusive mixed convection inside a ventilated two-dimensional square cavity filled with an air-CO_2 mixture. A uniform heat and CO_2 contaminant sources are applied on the bottom wall. The vertical and upper walls are fixed at external temperature and CO_2 concentration. An external fresh air enters at the cavity through an opening located at the top of the left vertical wall and exits from another one at the bottom of the opposite wall. The Reynolds and thermal Rayleigh numbers are fixed at 706 and 2.62×10^9, respectively. To study the CO_2 contaminant source's effect on the temperature distribution and indoor air quality, three different values of CO_2 amount are considered, viz., 1000, 2000 and 3000 ppm. The obtained results indicate that the increasing of CO_2 source does not influence the ventilation effectiveness for temperature distribution. This is due to the predominance of the thermal buoyancy forces driven by the heat source and the external forces caused by the ventilation. Nevertheless, its role remains important in terms of CO_2 distribution and index of indoor air quality.

Keywords: Mixed double-diffusive convection, Ventilation, Numerical simulation, Ventilated cavity, Turbulence Modeling.

Résumé:

Une étude numérique a été réalisée sur la convection mixte double diffusion en régime turbulent dans une cavité carrée bidimensionnelle ventilée et remplie d'un mélange air-CO_2. Une source de chaleur et de contamination en CO_2 uniforme a été appliquée sur la paroi inférieure. Les parois verticales ainsi que la paroi horizontale supérieure sont fixées à la température et à la concentration en CO_2 extérieures. Un écoulement d'air frais extérieur pénètre dans la cavité via une ouverture située au sommet de la paroi verticale gauche et sort à l'aide d'une autre ouverture placée au fond de la paroi opposée. Les nombres de Reynolds et de Rayleigh thermique sont fixés à 706 et 2.62×10^9, respectivement. Afin d'étudier l'effet de la source de contaminant sur la distribution de la température et la qualité de l'air intérieur, trois valeurs du montant en CO_2 ont été envisagées, à savoir 1000, 2000 et 3000 ppm. Les résultats obtenus ont montré que l'augmentation de la source de CO_2 n'a aucune influence sur l'efficacité de la ventilation à distribuer la température. Ceci est dû à la prédominance des forces de flottabilité thermique entraînées par la source de chaleur et des forces *extérieures provoquées par la ventilation. Néanmoins, son rôle reste important en termes de distribution du contaminant CO_2 et d'indice de qualité de l'air intérieur.*

Mots clefs: Convection mixte double diffusion, Ventilation, Simulation numérique, Cavité ventilée, Turbulence.

Nomenclature

C	Chemical species' concentration (*ppm*)
C_0	Reference concentration, $C_0 = (C_H + C_L)/2$ (*ppm*)
C_{Th}	Threshold concentration (*ppm*)
C_p	Specific heat ($J.Kg^{-1}.K^{-1}$)
C'	Fluctuating concentration (*K*)
D	Diffusion coefficient of chemical species ($m^2.s^{-1}$)
I	Intensity of turbulent kinetic energy, $I = \sqrt{k}$ ($m.s^{-1}$)
I_{IAQ}	Index of indoor air quality, $I_{IAQ} = (C_m - C_{out})/(C_{Th} - C_{out})$
g	Gravity acceleration ($m.s^{-2}$)
h	Height of the inlet or outlet air gap (*m*)
H, L	Cavity's height and width (*m*)
k	Turbulent kinetic energy ($m^2.s^{-2}$)
Le	Lewis number, $Le = \alpha_0/D$
n	Normal vector (*m*)
p	Fluid pressure (*Pa*)
Pr	Prandtl number, $Pr = \nu_0/\alpha_0$
Ra_T	Rayleigh number, $Ra_T = \rho_0 g \beta_T \Delta T L^3/(\mu_0 \alpha_0)$
Re	Reynolds number, $Re = \rho_0 U_{in} h_{in}/\mu_0$
T	Fluid temperature (*K*)
T_0	Reference temperature, $T_0 = (T_H + T_C)/2$ (*K*)
T'	Fluctuating temperature (*K*)
u, w	Horizontal and vertical velocities ($m.s^{-1}$)
u', w'	Fluctuating velocity components ($m.s^{-1}$)
U	Velocity modulus ($m.s^{-1}$)
$\vec{U}$	Velocity vector ($m.s^{-1}$)
x, z	Horizontal and vertical coordinates (*m*)
X, Z	Dimensionless coordinates, $(X, Z) = (x, z)/L$

Greek symbols

α	Thermal diffusivity ($m^2.s^{-1}$)
β_S	Solutal expansion coefficient, $\beta_S = C_0^{-1}$
β_T	Thermal expansion coefficient, $\beta_T = T_0^{-1}$ (K^{-1})
ε	Turbulent energy dissipation ($m^2 s^{-3}$)
ε_C	Ventilation effectiveness for the removal of pollutants, $\varepsilon_C = (C_{out} - C_{in})/(C_m - C_{in})$
ε_T	Ventilation effectiveness for temperature distribution, $\varepsilon_T = (T_{out} - T_{in})/(T_m - T_{in})$
ΔC	Characteristic concentration difference, $\Delta C = C_H - C_L$ (*ppm*)
ΔT	Characteristic temperature difference, $\Delta T = T_H - T_C$, (*K*)
λ	Thermal conductivity ($W.m^{-1}.K^{-1}$)
μ	Dynamic viscosity ($kg.m^{-1}.s^{-1}$)
ν	Kinematic viscosity ($m^2.s^{-1}$)
ρ	Density ($kg.m^{-3}$)

Superscripts/subscripts

C	Cold
H	Hot or high
in	Inlet
L	Low
m	Mean or average
out	Outlet
S	Solutal
T	Thermal
t	Turbulent
0	Reference

1 Introduction

In the last few years, indoor air quality (*IAQ*) has become of greater concern due to the increased amount of time people spend in indoor environments. It has been mentioned that many people spend more than *90%* of their time indoor such as homes, schools, offices, transports or shopping centers [1, 2]. The contaminant levels at indoor environments are typically much higher than that of outdoor environment [1]. More and more polluted products are being emitted by used building materials and furnishings, consumer and decoration products. Further, since the 1973 oil crisis, buildings have been sealed more tightly in order to reduce the energy consumption associated with heat losses [3]. Whereas such development was successful in certain respects (e.g., reducing costs), it also created other problems such as confinement and poorer air quality [3].

Increased awareness of the potential health risks associated with indoor air pollutants has stimulated interest to deepen our knowledge of how the ventilated air is distributed and how contaminants are transported within buildings. The indoor air movement is also an asset for thermal comfort. Therefore, it is necessary to study the distribution of the air in rooms. To improve the indoor air quality, the ventilation is as one of the promising solutions. Its principle is to renew sufficiently and permanently the exhaust air by fresh air unpolluted. Inside ventilated rooms, two physical phenomena can occur, viz the natural convection that is induced by the buoyancy forces in the presence of heat and contaminant sources, and the forced convection due to external forces in the presence of mechanical ventilation. The combination of these two phenomena leads to the mixed convection.

Two mechanical ventilation modes are widely used. These are as function of the air intake velocity: mixing ventilation where the air fresh is blown at high velocity (turbulent air jets) and the displacement ventilation where air is supplied at low velocity. The association of buoyancy forces to the second mode can generate mixed convection.

It is well known that double diffusive mixed convection in cavities has been the subject of intensive research due to its importance in various engineering and geophysical applications. This includes nuclear reactors, solar ponds, lakes and reservoirs, solar collectors, crystal growth [4], and so on. In the present work, we consider a ventilated cavity as a first approximation to predict the temperature and CO_2 contaminant distributions, and *IAQ* within ventilated rooms. To perform this, the steady Reynolds Averaged Navier-Stokes (*RANS*) equations are solved via the scStream code. To deal with turbulence, the *RNG* $k-\varepsilon$ model [5] was used, due to its reliability (see Fig. 2).

2 Computational analysis

2.1 Physical domain

Fig. 1 shows the considered problem along with Cartesian coordinate system. It is a 2D-ventilated cavity of dimensions $1.04\times1.04\ m^2$ (i.e. length and height). It should be noted that such a configuration has been employed by several researchers [6, 7] thanks to the availability of interesting and accurate experimental data [8] that can validate the implemented numerical simulations. Here the working fluid is an air-CO_2 mixture. A uniform temperature (T_H) and CO_2 concentration (C_H) are applied on the bottom wall. The other walls are fixed at external temperature (T_C) and CO_2 concentration (C_L), with $T_H > T_C$ and $C_H > C_L$. An external fresh air enters in the cavity at T_C and C_L via a port at the top of the left vertical wall and naturally exits from another at the bottom of the opposite wall. The air inlet velocity is fixed at $0.57\ m.s^{-1}$, which leads to $Re = 706$. The thermal Rayleigh number considered here is 2.62×10^9. Such a considered thermal and mass diffusivities (α and D) give a Lewis number equal to 1.47. The latter is defined as the ratio of thermal diffusivity to mass diffusivity ($Le = \alpha_0/D$). Note that the thermo-physical properties of the mixture were achieved using relationships advised by Poling et al. [9].

2.2 Governing equations

A steady state 2D-model is considered to analyze the double-diffusive flow in the whole cavity. The following assumptions were made in the mathematical model: a) the flow is turbulent, fully developed, and viscous, b) the working fluid (air-CO_2), is Newtonian and incompressible under the Boussinesq approximation, and c) the dissipation, pressure forces' work, and radiation are assumed to be negligible. In addition, the level of concentration of CO_2 is considered low (the amount of CO_2 is much lower than air (0.04%)). Based on these assumptions, the *RANS* equations can be expressed as:

$$\nabla.\vec{U}=0 \tag{1}$$

$$\nabla\left(\vec{U}\otimes\vec{U}\right)=-(1/\rho)\nabla p+\nabla.\left(\nu\nabla\vec{U}-\overline{u_i^{'}u_j^{'}}\right)+g\left[\beta_T\left(T-T_0\right)+\beta_S\left(C-C_0\right)\right]\vec{e} \tag{2}$$

$$\nabla.\left(T\vec{U}\right)=\nabla\left(\alpha\nabla T-\overline{u_i^{'}T^{'}}\right) \tag{3}$$

$$\nabla.\left(C\vec{U}\right)=\nabla\left(D\nabla C-\overline{u_i^{'}C^{'}}\right) \tag{4}$$

with $C^{'}$ is the fluctuating concentration, $T^{'}$ is the fluctuating temperature, $u_i^{'}$ and $u_j^{'}$ are the fluctuating velocity components, and i and j indicate the directions ($1\leq i, j\leq 2$).

The average Reynolds stresses $\overline{u_i^{'}u_j^{'}}$, the turbulent heat flux $\overline{u_i^{'}T^{'}}$ and the turbulent mass flux $\overline{u_i^{'}C^{'}}$ are modeled as follow:

$$\overline{u_i^{'}u_j^{'}}=-\nu_t S_{ij}+\left(2/3\right)k\delta_{ij}\ ;\ \overline{u_i^{'}T^{'}}=-\alpha_t\nabla T\ ;\ \overline{u_i^{'}C^{'}}=-D_t\nabla C \tag{5}$$

where $k=\overline{u_i^{'}u_j^{'}}/2$ is the turbulent kinetic energy, δ_{ij} is the Kronecker tensor, α_t and D_t are the turbulent thermal and mass diffusivities, respectively, and ν_t is the eddy viscosity which is computed by:

$$\nu_t=C_\mu k^2/\varepsilon \tag{6}$$

where ε is the turbulent dissipation rate, and C_μ is a constant model.

The *RNG k-ε* model which is an example of two equation models that use the Boussinesq conjecture is employed to close the system (1)-(4). It is based on the following equations:

$$\nabla.\left(k\vec{U}\right)=\nabla\left[\left(\nu+\left(\nu_t/\sigma_k\right)\right)\nabla k\right]+G_s+G_t+\varepsilon \tag{7}$$

$$\nabla.\left(\rho\varepsilon\vec{U}\right)=\nabla\left[\left(\nu+\left(\nu_t/\sigma_\varepsilon\right)\right)\nabla\varepsilon\right]+C_1\left(G_s+G_t\right)\left(1+C_3R_f\right)\left(\varepsilon/k\right)-C_2\left(\varepsilon^2/k\right) \tag{8}$$

with $G_s=\nu_t S_{ij}\nabla.\vec{U}$, $G_t=g_i\beta_T\left(\nu_t/Pr_t\right)\nabla T+g_i\beta_C\left(\nu_t/Sc_t\right)\nabla C$, $R_f=-G_t/\left(G_t+G_s\right)$, $S_{ij}=\overline{u}_{i,j}+\overline{u}_{j,i}$, and σ_k, σ_ε, C_1, C_2, C_3, C_μ are the model constants.

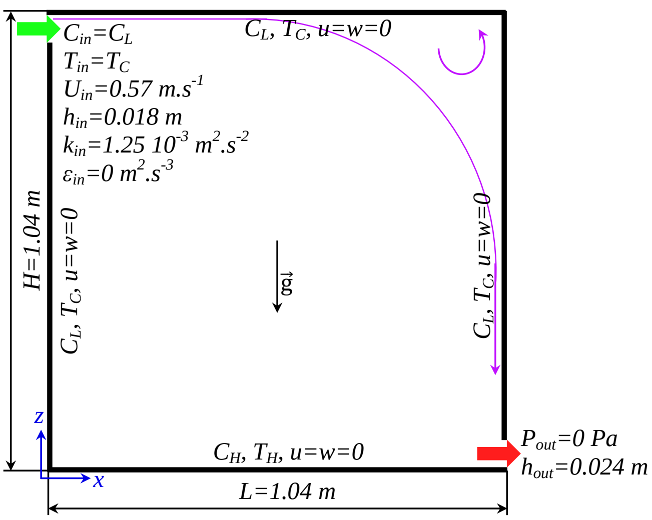

Fig. 1. Schematic diagram for the ventilated cavity with boundary conditions.

2.3 Boundary conditions

The appropriate boundary conditions (BCs) are: $u = w = 0$ (adherence), $u = u_{in}$ and $w = 0$ at the inlet, and $\partial(u,w)/\partial n = 0$ at the outlet. As for thermal BCs, $T_{in} = 288\ K$, $T_H = 308.5\ K$, $T_C = 288\ K$, and the temperature at the outlet level is $\partial T/\partial n = 0$. For the contaminant, $C_{in} = 350\ ppm$, at the floor C_H (varied between *1000* and *3000 ppm*), $C_L = 350\ ppm$, and at the outlet port $\partial C/\partial n = 0$. Regarding turbulent quantities, they are [8]: $k_{in} = 1.25\times10^{-3}\ m^2.s^{-2}$ and $\varepsilon_{in} = 0\ m^2.s^3$, and $\partial k/\partial n = 0$ and $\partial\varepsilon/\partial n = 0$ at outlet.

3 Numerical Procedure

3.1 Discretization

The abovementioned conservation equations (1)-(8), along with suitable BCs were discretized using the general purpose finite-volume method [10]. A quadratic structured mesh was used with a geometric expansion coefficient of *1.05* to the center of the cavity due to higher temperature, concentration and velocity gradients expected. The convective terms were handled by the *QUICK* scheme [11, 12] and diffusive terms were formulated using the second-order central differencing scheme [13]. The *SIMPLEC* algorithm was adopted for the pressure-velocity coupling. The resolution of the resulting algebraic system was achieved using multiple-iteration constrained conjugate gradient [14]. To ensure that the results are grid-independent and well-resolved, the simulations were repeated with different fine levels of meshing. It was determined that there are no noticeable differences in the solutions when the number of cells is around 196×196-cells or greater. The convergence criteria is set at 10^{-8} for the residual error of each variable that correspond to *1%* of the default tolerance settings.

3.2 Numerical verification

To check and validate our approach, the ventilated cavity under thermal Buoyancy force and turbulent flow regime reported by [8] was solved. The check and validation processes were presented by [7], with satisfactory results. Furthermore, the check process was completed considering the problem published by Zhang et al. [6] to perform a quantitative and qualitative numerical comparison between solutions. Fig. 2 depicts the obtained results in terms of temperature (T) and intensity of turbulent kinetic energy (I) at $X=0.5$. For the temperature prediction, the *LES* [15, 16], v^2-f [17] and *RNG* k-ε models corroborate the Blay et al.'s measurements [8]. From the predicted intensity of k, the *RNG* k-ε and v^2-f models were almost similar and corroborate experimental data. Regarding the LES model, there are significant deviations near walls. These are certainly due to the insufficient mesh size within boundary layers. Note that, here, the mesh size has been selected such that wall coordinate $y+$ values remain less than 5.

4 Results and discussions

Regarding the ventilation efficiency, the ventilation effectiveness for temperature distribution (ε_T), the pollutant removal effectiveness (ε_C) and index of *IAQ* (I_{IAQ}) are computed. These parameters are relevant to get an idea about the ventilation effectiveness to ensure the comfort of the occupants. They provide a quantitative index related to the way in which heat and pollutants are distributed all over inside the cavity, the higher the value the more homogeneous temperature and pollutants distributions. Awbi expresses these parameters as [18]:

$$\varepsilon_T = \frac{T_{out} - T_{in}}{T_m - T_{in}} \tag{9}$$

$$\varepsilon_C = \frac{C_{out} - C_{in}}{C_m - C_{in}} \tag{10}$$

$$I_{IAQ} = \frac{C_m - C_{out}}{C_{Th} - C_{out}} \tag{11}$$

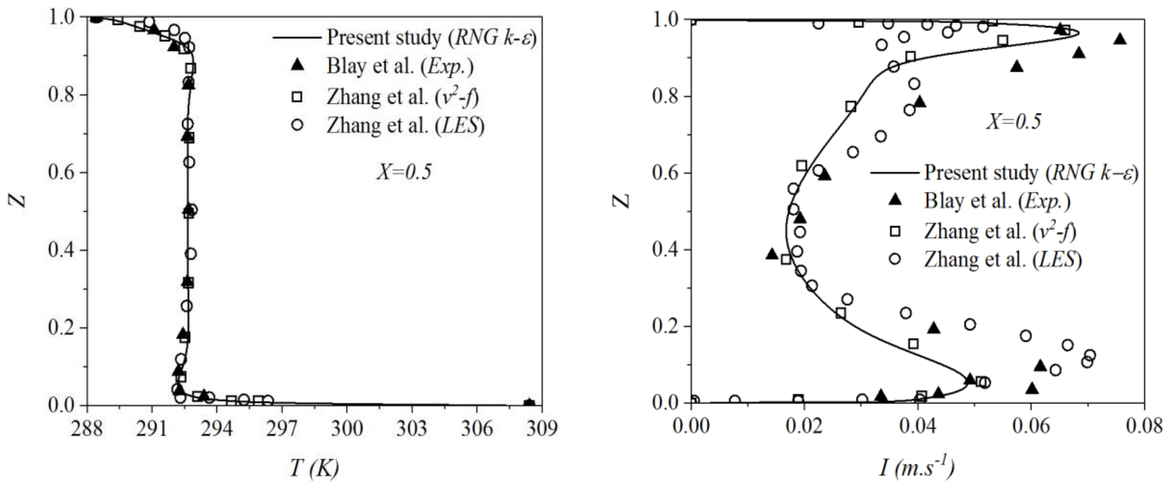

Fig. 2. Simulated and measured: temperature (left) and intensity of turbulent kinetic energy (right), on the centerline *X=0.5*; Comparison with Blay et al. [8] (*Exp.*) and Zhang et al. [6] (*Num.*).

Fig. 3 illustrates these parameters vs. C_H. It shows that ε_T is insensitive to the increasing of the CO_2 source due to its low values. That means the solutal buoyancy forces are negligible past the thermal buoyancy and external forces which are the motor of the motion. On the other hand, the value of ε_T is around *0.7*, this indicates that the ventilation does not allow sufficiently the heat to be evacuated. Regarding the pollutant removal effectiveness, we found that ε_C evolves with C_H. As we can see, its values remain less than unity. This denotes that the ventilation process does not sufficiently evacuate the CO_2 contaminant. As for I_{IAQ}, it increases with C_H, but always less than unity, which means that *IAQ* is ensured compared to the advocated threshold CO_2 concentration (*1000 ppm*).

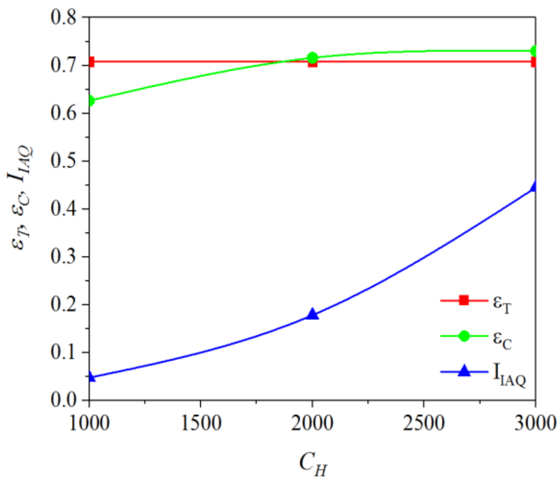

Fig. 3. Ventilation effectiveness for temperature distribution (ε_T), ventilation effectiveness for the removal of CO_2 (ε_C), and index of *IAQ* (I_{IAQ}) vs. C_H.

Based on the obtained results, we can state that the ventilation process upholds acceptable temperature and CO_2 contaminant distributions, despite low values of ε_T and ε_C. Thereby, these can be used in temperate climate zones (e.g. a Mediterranean climate) to insure a good *IAQ* and maintain an appreciable temperature level.

5 Conclusion

The turbulent double-diffusive mixed convection flow in a 2D-model was computationally investigated. The emphasis has been on the influence of CO_2 contaminant source on the temperature distribution and indoor air quality inside a ventilated room filled with air-CO_2. Simulations have been performed with thermal Rayleigh number of 2.62×10^9, Reynolds number of *706*, Prandtl number of *0.71*, Lewis number of *1.47*, and various CO_2 source between *1000* and *3000 ppm*. In steady RANS equations, the *RNG k-ε* turbulence model was used. From the obtained results, it can be concluded that the increasing of CO_2 source does not affect the ventilation effectiveness for temperature distribution parameter. This explains that the solutal buoyancy force driven by the CO_2 concentration gradients can be neglected at the building scale due to the low values of CO_2 (seldom exceed *3000 ppm*), but still remains dangerous for occupants' health. It is recommended to consider its effect on industrial applications where the concentrations are heavy (e.g. combustion process). Though, the considered ventilation process insures a good indoor air quality, since $I_{IAQ} < 1$ as long as $C_H < 3000$ *ppm*.

References

[1] A.P. Jones, Indoor air quality and health, Atmos. Environ. 33 (1999) 4535-4564.

[2] Q.-H. Deng, J. Zhou, C. Mei, Y.-M. Shen, Fluid, heat and contaminant transport structures of laminar double-diffusive mixed convection in a two-dimensional ventilated enclosure, Int. J. Heat Mass Transf. 47 (2004) 5257-5269.

[3] E. Kabir, K.-H. Kim, J.R. Sohn, B.Y. Kweon, J.H. Shin, Indoor air quality assessment in child care and medical facilities in Korea, Environ. Monit. Assess. 184 (2012) 6395-6409.

[4] S. Saha, M.N. Hasan, I.A. Khan, Double diffusive mixed convection heat transfer inside a vented square cavity, Chem. Eng. Res. Bull. 13 (2009) 17-24.

[5] V. Yakhot, S.A. Orszag, S. Thangam, T.B. Gatski, C.G. Speziale, Development of turbulence models for shear flows by a double expansion technique, Phys. Fluids 4 (1992) 1510-1520.

[6] Z. Zhang, W. Zhang, Z.J. Zhai, Q.Y. Chen, Evaluation of various turbulence models in predicting airflow and turbulence in enclosed environments by CFD: Part 2-Comparison with experimental data from literature, HVACR Res. 13 (2007) 871-886.

[7] L. Koufi, Z. Younsi, Y. Cherif, H. Naji, Numerical investigation of turbulent mixed convection in an open cavity: Effect of inlet and outlet openings, Int. J. Therm. Sci. 116 (2017) 103-117.

[8] D. Blay, S. Mergui, C. Niculae, Confined turbulent mixed convection in the presence of a horizontal buoyant wall jet, Fundamentals Mixed Convection, Heat Transfer Div. 213 (1992) 65-72.

[9] B.E. Poling, J.M. Prausnitz, J.P. O'connell, The properties of gases and liquids, Mcgraw-hill, New York, 2001.

[10] S. Patankar, Numerical heat transfer and fluid flow, Hemisphere publishing, Washington, 1980.

[11] B.P. Leonard, A stable and accurate convective modelling procedure based on quadratic upstream interpolation, Comput. Methods Appl. Mech. Eng. 19 (1979) 59-98.

[12] T. Hayase, J.A.C. Humphrey, R. Greif, A consistently formulated QUICK scheme for fast and stable convergence using finite-volume iterative calculation procedures, J. Comput. Phys. 98 (1992) 108-118.

[13] A. Kurganov, E. Tadmor, New high-resolution central schemes for nonlinear conservation laws and convection-diffusion equations, J. Comput. Phys. 160 (2000) 241-282.

[14] I. Gustafsson, A class of first order factorization methods, BIT Numer. Math. 18 (1978) 142-156.

[15] M. Germano, U. Piomelli, P. Moin, W.H. Cabot, A dynamic subgrid- scale eddy viscosity model, Phys. Fluids Fluid Dyn. 3 (1991) 1760-1765.

[16] D.K. Lilly, A proposed modification of the Germano subgrid- scale closure method, Phys. Fluids Fluid Dyn. 4 (1992) 633-635.

[17] L. Davidson, P.V. Nielsen, A. Sveningsson, Modifications of the v^2-f model for computing the flow in a 3D wall jet, Turbulent Heat Mass Transfer 4 (2003) 577-584.

[18] H.B. Awbi, Ventilation of buildings, 2nd ed., Routledge, London, New York, 2003.